The Astrophysical Journal, 647:1531–1534, 2006 August 20

THE ^1D–^3P TRANSITIONS IN ATOMIC OXYGEN INDUCED BY IMPACT WITH ATOMIC HYDROGEN

R. V. Krems
Department of Chemistry, University of British Columbia, Vancouver, BC V6T 1Z3, Canada; rkrems@chem.ubc.ca

M. J. Jamieson
Department of Computing Science, University of Glasgow, Glasgow G12 8QQ, Scotland

and

A. Dalgarno
ITAMP, Harvard-Smithsonian Center for Astrophysics, Cambridge, MA 02138
Received 2006 February 10; accepted 2006 April 4

ABSTRACT

The rate coefficients for electronic transitions between the ^3P and ^1D states of oxygen atoms induced by collision with hydrogen atoms are computed using a rigorous quantum mechanical method and accurate interaction potentials of the OH molecule. The rate coefficient for the electronic relaxation of O(^1D) to O(^3P) is almost independent of temperature between 1000 and 10,000 K with a magnitude of 10^{-12} cm^3 s^{-1}. The rate coefficient for the electronic excitation of O(^3P) to O(^1D) varies from 5.40×10^{-23} cm^3 s^{-1} at $T = 1000$ K to 5.96×10^{-14} cm^3 s^{-1} at $T = 10{,}000$ K.

Subject headings: atomic data — atomic processes

Online material: color figure

1. INTRODUCTION

The excitation of ground state ^3P oxygen atoms to the metastable ^1D state in collisions with hydrogen atoms

$$\mathrm{O}\left(^3P\right) + \mathrm{H} \rightarrow \mathrm{O}\left(^1D\right) + \mathrm{H} \qquad (1)$$

is a potential source of the emission of the oxygen red lines at 630.0 and 636.4 nm in warm gases found in Herbig-Haro objects (Schwartz 1983), planetary nebulae (Pottasch 1984), supernova remnants (Raymond 1984), supernova ejecta, photon-dominated regions, stellar atmospheres, and comets (see also Pequignot [1990] and references therein). During magnetically disturbed conditions, protons precipitate into the terrestrial atmosphere. As they slow down, they capture electrons from the neutral constituents, and near the end of their trajectories, the hydrogen atoms may excite the ambient oxygen atoms to the metastable state, which, if not quenched in collisions with N_2 and O_2, will radiate, providing a diagnostic of the event. The reverse reaction to that in equation (1),

$$\mathrm{O}\left(^1D\right) + \mathrm{H} \rightarrow \mathrm{O}\left(^3P\right) + \mathrm{H}, \qquad (2)$$

may occur in environments in which metastable atoms are produced in reactions initiated by photons or electrons. If so, the red lines may be quenched and the reaction in equation (2) is a source of energetic hydrogen and oxygen atoms.

The electronic relaxation of O(^1D) atoms in collisions with several atomic and molecular partners has been investigated experimentally (Streit et al. 1976; Matsumi & Chowdhury 1996), although not with atomic hydrogen. The process in equation (1) has been studied theoretically by Federman & Shipsey (1983), who employed the Landau-Zener approximation. They obtained estimates of rate coefficients that they believed to be accurate to within an order of magnitude. The molecular parameters that enter the Landau-Zener approximation and control the collision process have been determined subsequently with much greater precision (van Dishoeck & Dalgarno 1983; Yarkony 1992; Parlant & Yarkony 1999; X. Chu 2004, private communication), and a more rigorous study using multichannel scattering theory is warranted.

In the excitation process, the O(^3P) and H atoms approach along the potential energy curves of the $X^2\Pi$, $^2\Sigma^-$, $^4\Sigma^-$, and $^4\Pi$ states of the OH molecule with probabilities of 2/9, 1/9, 2/9, and 4/9, respectively, and separate along the $A^2\Sigma^+$, $2^2\Pi$, and $^2\Delta$ potential energy curves with probabilities determined by the spin-orbit and Coriolis interactions. The potentials of the $2^2\Pi$ and $^2\Delta$ states (van Dishoeck & Dalgarno 1983) and the $A^2\Sigma^+$, $X^2\Pi$, $^2\Sigma^-$, $^4\Sigma^-$, and $^4\Pi$ states (Yarkony 1992; Parlant & Yarkony 1999) are reproduced in Figure 1. Yarkony (1992) and Parlant & Yarkony (1999) carried out an elaborate quantum-mechanical calculation and analysis of the coupling matrix elements between the $A^2\Sigma^+$ state and the lower electronic states of the molecule in order to study the predissociation of OH($A^2\Sigma^+$).

In this work, we use the results of van Dishoeck & Dalgarno (1983) and Parlant & Yarkony (1999) to develop the methodology for quantum mechanical calculations of the rate coefficients for the processes in equations (1) and (2) and report the results of our computations.

2. SCATTERING THEORY

The Hamiltonian of the O-H collision system can be written (in atomic units) in the form

$$H = -\frac{1}{2\mu R}\frac{\partial^2}{\partial R^2}R + V_{\mathrm{cf}} + V_{\mathrm{nr}} + V_{\mathrm{so}}, \qquad (3)$$

where R is the internuclear distance, μ is the reduced mass, V_{nr} is the nonrelativistic electrostatic interaction, V_{so} is the spin-orbit interaction, and $V_{\mathrm{cf}} = \boldsymbol{l}^2/2\mu R^2$ is the centrifugal interaction arising from the angular motion of the nuclei, where $\boldsymbol{l}$ is the rotational angular momentum of the nuclei. The electronic states of the separated atoms are specified by the quantum numbers of the

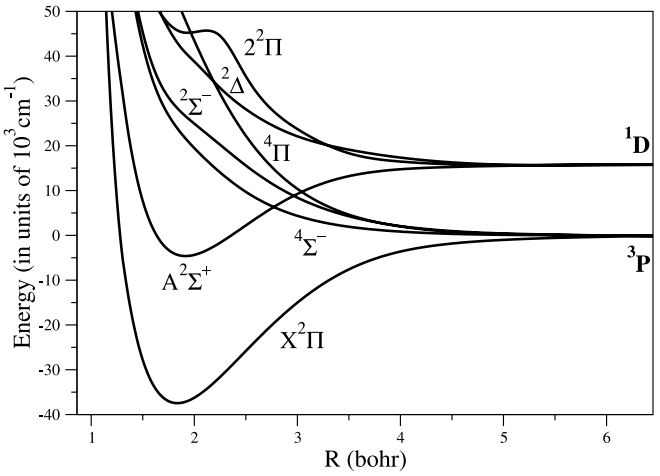

FIG. 1.—Interatomic potential energy curves of OH. [*See the electronic edition of the Journal for a color version of this figure.*]

electronic orbital $\boldsymbol{L}$ and spin $\boldsymbol{S}_{\rm O}$ angular momenta of oxygen and the electronic spin angular momentum $\boldsymbol{S}_{\rm H}$ of hydrogen. The vector sum of $\boldsymbol{L}$ and $\boldsymbol{S}_{\rm O}$ gives the total angular momentum of oxygen $\boldsymbol{j}_{\rm O}$, and the total angular momentum of hydrogen is $j_{\rm H} = S_{\rm H} = 1/2$. The vector sum $\boldsymbol{j} = \boldsymbol{j}_{\rm O} + \boldsymbol{j}_{\rm H}$ yields the total electronic angular momentum of the OH molecule. The total angular momentum $\boldsymbol{J} = \boldsymbol{j} + \boldsymbol{l}$ and its projection M are conserved. The electronic spin angular momentum of oxygen is $S_{\rm O} = 1$ in the $L = 1$ state (^3P) and $S_{\rm O} = 0$ in the $L = 2$ state (^1D).

For each value of J and M, we expand the eigenfunctions of the Hamiltonian in equation (3) as

$$\Psi^{JM} = \sum_j \sum_l \sum_{j_{\rm O}} \sum_L |JMjlj_{\rm O}L\rangle F^J_{jlj_{\rm O}L}(R), \qquad (4)$$

where $F_{jlj_{\rm O}L}(R)$ are functions of R and $|JMjlj_{\rm O}L\rangle$ are coupled atomic wave functions. They are related to Hund's case (a) basis functions $|JM\Lambda S\Sigma\rangle$, where S is the total spin of the molecule and Λ and Σ are the projections of $\boldsymbol{L}$ and $\boldsymbol{S}$ on the interatomic axis (Singer et al. 1983). At $R = \infty$, the relations are

$$|JMjlj_{\rm O}L\rangle = \sum_\Lambda \sum_S \sum_\Sigma |JM\Lambda S\Sigma\rangle (-1)^{l-J-\Omega}[(S)(j_{\rm H})(j_{\rm O})(L)]^{1/2} \times \langle j - \Omega J\Omega | l0\rangle \langle L\Lambda S\Sigma | j\Omega\rangle \begin{Bmatrix} L & S_{\rm O} & j_{\rm O} \\ 0 & S_{\rm H} & j_{\rm H} \\ L & S & j \end{Bmatrix}, \qquad (5)$$

where $\Omega = \Lambda + \Sigma$, the symbols in the angle brackets are Clebsch-Gordan coefficients, the symbol in the curly brackets is a 9j-symbol and (X) is an abbreviation for $(2X + 1)$. The matrix elements of the Hamiltonian in the total angular momentum representation are independent of M, so we omit it from the equations.

Substitution of the expansion (eq. [4]) in the Schrödinger equation with the Hamiltonian (eq. [3]) results in a set of coupled differential equations determined by the electrostatic, spin-orbit, and centrifugal interactions. The matrix of the $\boldsymbol{l}^2$ operator is diagonal in the $|Jjlj_{\rm O}L\rangle$ basis at $R = \infty$, and the spin-orbit interaction $V_{\rm so}$ couples the $L = 1$ and $L = 2$ states of atomic oxygen. Therefore, the scattering S-matrix cannot be constructed from the solution of the Schrödinger equation directly in the $|Jjlj_{\rm O}L\rangle$ representation. To satisfy the boundary conditions, we introduce a transformation matrix $\mathbf{C}$ that diagonalizes the matrix of the spin-orbit interaction at $R = \infty$ and we solve the differential equations

$$\left(\frac{d^2}{dR^2} + 2\mu E\right) F^J_\alpha(R) = 2\mu \sum_{\alpha'} \left[\mathbf{C}^T \mathbf{U} \mathbf{C}\right]_{\alpha;\alpha'} F^J_{\alpha'}(R), \qquad (6)$$

where E is the total energy and $\mathbf{U}$ is the sum of the matrices $\mathbf{V}_{\rm nr}$, $\mathbf{V}_{\rm so}$, and $\mathbf{V}_{\rm cf}$ in the $|Jjlj_{\rm O}L\rangle$ representation. The symbol α denotes the eigenstates of the $\mathbf{U}$ matrix in the $R = \infty$ limit. The coefficients F_α are related to the coefficients $F_{jlj_{\rm O}L}$ by the transformation $\mathbf{C}$.

The spin-orbit coupling strength between the $L = 1$ and $L = 2$ states of oxygen is of the order of 100 cm^{-1}, compared to the ^1D–^3P energy difference of 15868 cm^{-1}, so we may continue to label the states by L, even though it is not a good quantum number. The transformation matrix $\mathbf{C}$ is obtained by a numerical diagonalization of $\mathbf{U}$ at $R = \infty$. A similar procedure has been used in the theory of collisions in external magnetic fields (Krems & Dalgarno 2004).

To calculate the matrix $\mathbf{U}$, we construct the matrices $\mathbf{V}_{\rm nr}$, $\mathbf{V}_{\rm so}$, and $\mathbf{V}_{\rm cf}$ in the molecular Hund's case (a) basis and transform them to the $|Jjlj_{\rm O}L\rangle$ basis using equation (5). The matrix of the $V_{\rm nr}$ operator is diagonal in the molecular basis $|\Lambda S\Sigma\rangle$ with the OH potentials of Figure 1 as elements. An alternative theory may be based on the expansion of the electrostatic interaction potential in spherical tensors, which would yield the matrix elements of the interaction potential in the coupled basis directly (Krems et al. 2004). The matrix elements of $\boldsymbol{l}^2$ are obtained from the relation

$$\boldsymbol{l}^2 = \boldsymbol{J}^2 + \boldsymbol{L}^2 + \boldsymbol{S}^2 + 2\boldsymbol{L}_z\boldsymbol{S}_z - 2\boldsymbol{J}_z\boldsymbol{L}_z - 2\boldsymbol{J}_z\boldsymbol{S}_z + \boldsymbol{L}_+\boldsymbol{S}_- + \boldsymbol{L}_-\boldsymbol{S}_+ - \boldsymbol{J}_+(\boldsymbol{L}_- + \boldsymbol{S}_-) - \boldsymbol{J}_-(\boldsymbol{L}_+ + \boldsymbol{S}_+), \qquad (7)$$

where $\boldsymbol{L}_z$, $\boldsymbol{S}_z$, and $\boldsymbol{J}_z$ are the z-components of the electronic orbital and spin and molecular total angular momenta and $\boldsymbol{L}_\pm$, $\boldsymbol{S}_\pm$, and $\boldsymbol{J}_\pm$ are the raising and lowering operators. The matrix elements of all operators in equation (7) are known at $R = \infty$. Parlant & Yarkony (1999) calculated the matrix elements of the $\boldsymbol{L}_+$ operator between the $^4\Pi$ and $^4\Sigma^-$ states, the $X^2\Pi$ and $A^2\Sigma^+$ states, and the $X^2\Pi$ and $^2\Sigma^-$ states as functions of R. We used their values. For the other elements of the $\boldsymbol{l}^2$ matrix, we adopted the values at $R = \infty$.

At infinite interatomic separation, the nonzero matrix elements of $V_{\rm so}$ are given by

$$\langle Jjlj_{\rm O}L|V_{\rm so}|Jj'l'j'_{\rm O}L'\rangle = \delta_{ll'}\delta_{jj'}\delta_{j_{\rm O}j'_{\rm O}}\delta_{LL'}\delta_{L1}\Delta_{j_{\rm O}}, \qquad (8)$$

$$\langle Jjlj_{\rm O}L|V_{\rm so}|Jj'l'j'_{\rm O}L'\rangle = \delta_{ll'}\delta_{jj'}\delta_{j_{\rm O}j'_{\rm O}}\delta_{j_{\rm O}2}\delta_{L1}\delta_{L'2}\Delta(L,\ L'). \qquad (9)$$

Parlant & Yarkony (1999) computed the part of the spin-orbit interaction matrix $V_{\rm so}$ in the Hund's case (a) basis involving four molecular states correlating with the ^3P–^2S atomic threshold and the $A^2\Sigma^+$ state. We have chosen $\Delta_{j_0=2} = -75$ cm^{-1}, $\Delta_{j_0=1} = 75$ cm^{-1}, $\Delta_{j_0=0} = 150$ cm^{-1}, and $\Delta(L,\ L') = 100$ cm^{-1}, which reproduces all matrix elements computed by Parlant & Yarkony at $R = 10$ bohr to within 2.1% of their absolute magnitude. The signs of several matrix elements of Parlant & Yarkony (1999) are inconsistent with the transformation in equation (5). The differences are summarized in the Appendix.

3. RESULTS

Equation (6) is a set of 28 coupled differential equations. We solved them numerically on the radial grid $R = 0-100$ Å of 10,000 points for 2000 collision energies in the interval from 10

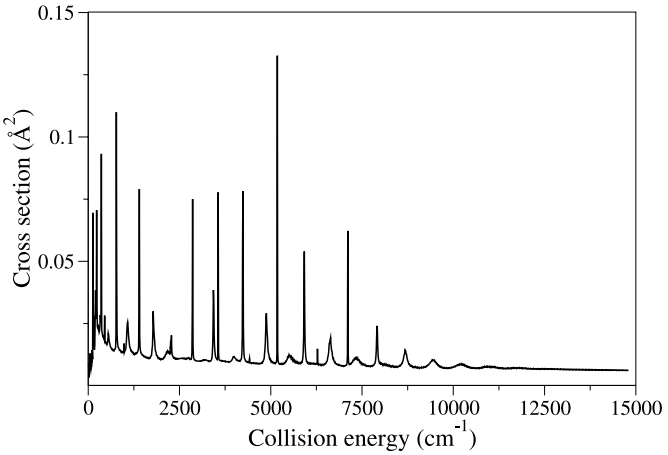

FIG. 2.—Cross section for the $^1D \rightarrow {}^3P$ relaxation as a function of collision energy.

to 20,000 cm^{-1} and 96 values of the total angular momentum $J = 4.5-100.5$. To verify the accuracy of our calculations, we used the log-derivative propagator of Johnson (1973) and Manolopoulos (1986) and the Numerov method to integrate the differential equations. In Figure 2 we show the energy dependence of the cross section for the reaction given in equation (2) as a function of energy. Many shape resonances occur for energies below 1.24 eV. Most are narrow and individually enhance the cross section by less than an order of magnitude. Their contribution to the thermal rate coefficient is not significant. In Figure 3 we show the rate coefficient k_q as a function of temperature T obtained by averaging the product of the cross section and the relative velocity over a Maxwellian velocity distribution. At temperatures between 1000 and 10,000 K, it may be represented in units of cm^3 s^{-1} with the accuracy of 1% by the expression

$$k_q(T) = \frac{(1.74T/6000 + 0.06)10^{-12}}{\sqrt{T/6000}} \exp(-0.47T/6000). \quad (10)$$

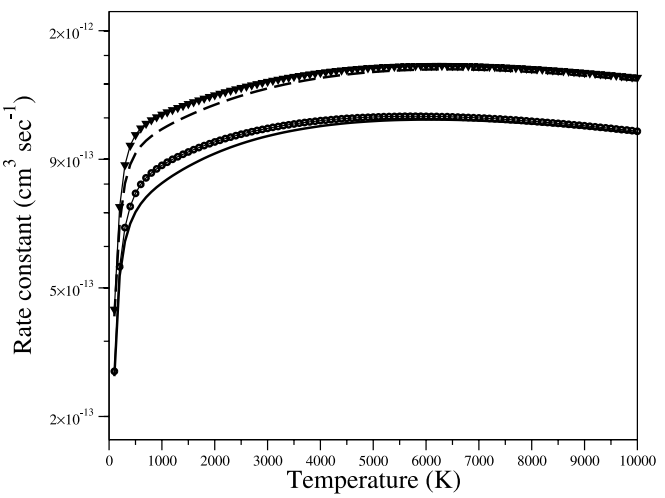

FIG. 3.—Rate coefficients for the $^1D \rightarrow {}^3P$ transition in collisions of oxygen and hydrogen as functions of temperature. *Solid line:* rigorous calculation; *circles:* calculations assuming the matrix element of $\boldsymbol{l}^2$ are constant (independent of the interatomic distance); *dashed line:* calculations assuming the spin-orbit interaction is constant; *triangles:* calculations assuming both the $\boldsymbol{l}^2$ and spin-orbit interaction matrix elements are constant.

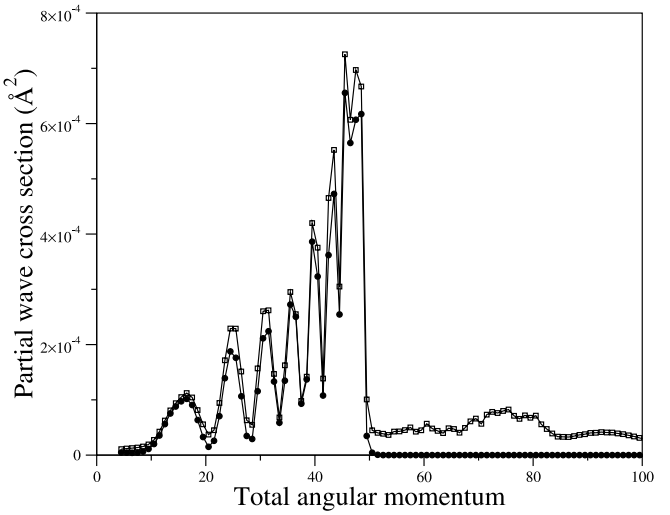

FIG. 4.—Partial wave cross sections for the $^1D \rightarrow {}^3P$ transition at a collision energy of 1.24 eV as functions of total angular momentum J. *Circles:* rigorous calculation; *squares:* calculations without the transformation **C** in eq. (6).

To identify the principal mechanism for the $^1D \leftrightarrow {}^3P$ transition, we repeated the calculations, neglecting the radial dependence of the matrix elements of the $\boldsymbol{l}^2$ operator between the states separating to the ^3P and ^1D atomic limits. The results are shown in Figure 3. The rate coefficients are nearly unchanged, indicating that the $^1D \leftrightarrow {}^3P$ transition is driven by the spin-orbit interaction. Another frequent approximation is the assumption that the spin-orbit interaction is independent of R. We found, as shown in Figure 3, that it leads to an overestimate by a factor of 1.4 in the high-temperature regime. It is important to include the diagonalizing transformation matrix **C** in equation (6). Figure 4 presents the partial wave cross sections at an energy of 1.24 eV for individual values of the total angular momentum J when we apply **C** and when we do not. Without **C**, there occurs a substantial accumulation of artificial amplitudes for the transition at large internuclear distances despite the high centrifugal barriers. The transformation suppresses them. The integral cross section computed without the transformation **C** at 1.24 eV overestimates the accurate result by about 55%.

Numerical values of the quenching rate coefficient are given in Table 1. It increases rapidly from 2.8×10^{-13} cm^3 s^{-1} at

TABLE 1

RATE COEFFICIENTS FOR THE PROCESSES IN EQUATIONS (1) AND (2), IN UNITS OF cm^3 s^{-1}

Temperature (K)	k_q	$k_{\rm exc}$
100	2.83×10^{-13}	...
200	4.85×10^{-13}	...
300	5.84×10^{-13}	...
500	6.84×10^{-13}	...
700	7.41×10^{-13}	2.81×10^{-27}
1000	8.00×10^{-13}	5.40×10^{-23}
2000	9.38×10^{-13}	5.74×10^{-18}
3000	1.03×10^{-12}	2.83×10^{-16}
4000	1.09×10^{-12}	2.01×10^{-15}
5000	1.12×10^{-12}	6.47×10^{-15}
6000	1.13×10^{-12}	1.40×10^{-14}
7000	1.12×10^{-12}	2.39×10^{-14}
8000	1.10×10^{-12}	3.52×10^{-14}
10,000	1.05×10^{-12}	5.96×10^{-14}

$T = 100$ K to 1.0×10^{-12} cm^3 s^{-1} at 2700 K and varies slowly thereafter. The rate coefficients agree[1] to within a factor of 1.5 with the values obtained by Federman & Shipsey (1983). Rate coefficients $k_{\rm exc}$ for the excitation process in equation (1) may be obtained from the formula

$$k_{\rm exc} = \frac{g_D}{g_P} e^{-\Delta\epsilon/k_{\rm B}T} k_q, \qquad (11)$$

where $g_D = 10$ and $g_P = 18$ are statistical weights, $\Delta\epsilon$ is the energy separation between the ^3P and ^1D states of oxygen equal to 15867.86 cm^{-1}, and $k_{\rm B}$ is the Boltzmann constant. Neglecting the energy difference between the fine structure levels of O(^3P), we find the rate constants 5.40×10^{-23} cm^3 s^{-1} at $T = 1000$ K and 5.96×10^{-14} cm^3 s^{-1} at $T = 10{,}000$ K for the electronic excitation of O(^3P). In low-density regions of interstellar space, most oxygen atoms are in the $^3P_2$ state. If oxygen is present in a distribution of fine structure levels, the effective excitation rate coefficients may be estimated from the quenching rate coefficient using the average energy difference between the ^3P and ^1D states. We have found that the excitation rate computed using equation (11) with $\Delta\epsilon = 15{,}790$ cm^{-1} at $T = 1000$ K exceeds the value presented in Table 1 by 10%, and at temperatures above 6000 K the difference is less than 1%.

[1] There is a measure of chance in this close agreement. The molecular parameters are different and the Landau-Zener formula for the transition probability at the avoided crossing used by Federman and Shipsey has an error of a factor of π. The calculation with the correct formula and updated values of the parameters yields rate coefficients that agree with our results to within the order of magnitude claimed by Federman and Shipsey.

We are grateful to D. Yarkony and S. R. Federman for helpful comments and to Peng Zhang for pointing out a misprint in equation (7). We thank Mark van der Loo and Gerrit Groenenboom of Radboud University Nijmegen for verifying most of the phase corrections in the Appendix. The work was supported by the University of British Columbia, the National Science Foundation grant ATM 04-30506, and a grant from the Institute for Theoretical, Atomic, Molecular and Optical Physics at the Harvard-Smithsonian Center for Astrophysics.

APPENDIX

SIGNS OF THE COUPLING MATRIX ELEMENTS

The phase of some matrix elements computed by Parlant & Yarkony (1999) is inconsistent with the transformation in equation (5) used in the present work. The following changes were made in Tables I and II and the appendix of Parlant & Yarkony (1999).

Table I: The matrix element $(1^4\Pi_{1/2},\ 1^2\Sigma^-_{1/2})$ must be positive. The sign of the matrix elements $(1^4\Pi_{1/2},\ A^2\Sigma^+_{1/2})$, $(X^2\Pi_{1/2},\ A^2\Sigma^+_{1/2})$, $(1^4\Sigma^-_{1/2}, A^2\Sigma^+_{1/2})$ and $(1^2\Sigma^-_{1/2}, A^2\Sigma^+_{1/2})$ depends of the sign of the matrix element $\Delta(L,\ L')$ in equation (9) of the present paper. The choice of the sign of $\Delta(L,\ L')$ is arbitrary, which we have confirmed by the calculations with both the positive and the negative signs of $\Delta(L,\ L')$ yielding identical results. If $\Delta(L,\ L')$ is chosen to be positive, the matrix elements $(1^4\Pi_{1/2},\ A^2\Sigma^+_{1/2})$ and $(1^4\Sigma^-_{1/2},\ A^2\Sigma^+_{1/2})$ must be positive and the matrix elements $(X^2\Pi_{1/2},\ A^2\Sigma^+_{1/2})$ and $(1^2\Sigma^-_{1/2},\ A^2\Sigma^+_{1/2})$ must be negative.

Table II: The matrix element $L^+(X^2\Pi_{3/2},\ 1^2\Sigma^-_{1/2})$ must be positive.

Appendix: The matrix element $(1^4\Pi_{1/2},\ 1^4\Sigma^-_{1/2})$ must be $+C$, the matrix element $(1'^4\Pi_{1/2},\ 1^2\Sigma^-_{1/2})$ must be $-(1/\sqrt{3})D$, and the matrix element $(1'^4\Pi_{1/2},\ A^2\Sigma^+_{1/2})$ must be $+(1/\sqrt{3})H$.

REFERENCES

Federman, S. R., & Shipsey, E. J. 1983, ApJ, 269, 791
Johnson, B. R. 1973, J. Comput. Phys., 13, 445
Krems, R. V., & Dalgarno, A. 2004, J. Chem. Phys., 120, 2296
Krems, R. V., Groenenboom, G. C., & Dalgarno, A. 2004, J. Phys. Chem. A, 108, 8941
Manolopoulos, D. E. 1986, J. Chem. Phys., 85, 6425
Matsumi, Y., & Chowdhury, A. M. S. 1996, J. Chem. Phys., 104, 7036
Parlant, G., & Yarkony, D. R. 1999, J. Chem. Phys., 110, 363
Pequignot, D. 1990, A&A, 231, 499
Pottasch, S. R. 1984, Planetary Nebulae (Dordrecht: Reidel)
Raymond, J. C. 1984, ARA&A, 22, 75
Schwartz, R. D. 1983, ARA&A, 21, 209
Singer, S. J., Freed, K. F., & Band, Y. B. 1983, J. Chem. Phys., 79, 6060
Streit, G. E., Howard, C. J., Schmeltekopf, A. L., Davidson, J. A., & Schiff, H. I. 1976, J. Chem. Phys., 65, 4761
van Dishoeck, E. F., & Dalgarno, A. 1983, J. Chem. Phys., 79, 873
Yarkony, D. R. 1992, J. Chem. Phys., 97, 1838